ChemPubSoc Europe

DOI: 10.1002/slct.201800229

Chemistry SELECT Communications

Electro, Physical & Theoretical Chemistry

# Adsorption and Decomposition of DMMP on Size-Selected $(WO_3)_3$ Clusters

Xin Tang[+],[a] Zachary Hicks[+],[a] Gerd Ganteför,[b] Bryan W. Eichhorn,[c] and Kit H. Bowen*[a]

The adsorption and decomposition behaviors of dimethyl methylphosphate (DMMP) on size-selected $(WO_3)_3$ clusters were studied by a combination of X-ray Photoelectron Spectroscopy (XPS) and Temperature Programmed Reaction (TPR). The fate of DMMP adsorbed on $(WO_3)_3$ clusters was found to be very similar to its fate on $(MoO_3)_3$. In contrast to DMMP on $(MoO_3)_3$, however, dimethyl ether was observed as a product in the reaction of DMMP with $(WO_3)_3$, in addition to methanol, due to the higher Lewis acidity of $(WO_3)_3$ clusters as compared to $(MoO_3)_3$.

The surface chemistry of chemical warfare agents is of critical importance to the rational design of sensors to detect chemical warfare agents and sorbents to decontaminate them.[1] Organophosphorus compounds are commonly used as chemical warfare agents,[2] and therefore, the adsorption and decomposition behaviors of organophosphates are widely studied by many research groups.[3] Of all the organophosphates, dimethyl methylphosphate (DMMP) has attracted considerable attention, since it has a similar structure to many nerve agents but a much lower toxicity, allowing for easier study. Thus, DMMP is frequently used as a structural simulant in many related studies of chemical warfare agents.[2,4]

Using DMMP as a model molecule, the reactivity of many metals and metal oxides toward DMMP has been studied, i.e. $MoO_3$,[5] Cu,[6] CuO,[7] MgO,[8] ZnO,[9] $CeO_2$,[4f] $TiO_2$,[4c] $Y_2O_3$[10]etc.. As illustrated in these studies, DMMP usually undergoes a stepwise loss of methoxy groups on the metal oxide surface, resulting in methanol being observed as a common hydrolysis reaction product for DMMP on many oxide surfaces.[11] In addition to the hydrolysis reaction, reduction processes are also observed when surface defects, i.e. oxygen vacancies, are present.[4c] It has also been noted that both the acidity and reducibility of metal oxides are known to affect the adsorption behavior and the decomposition pathway of DMMP molecules.[7,12] The acidity of metal oxides can affect the binding strength of the DMMP molecule to Lewis and/or Brønsted acid sites on the surface of metal oxides, while the reducibility of metal oxides enables the production of oxygen vacancies, which act as potential active sites to decompose DMMP molecules via a redox mechanism.[7]

In this work, the adsorption and decomposition behaviors of DMMP on tungsten oxide trimer clusters, $(WO_3)_3$ were studied via a combination of X-ray Photoelectron Spectroscopy (XPS) and Temperature Programmed Reaction (TPR). Prior work has been performed studying the adsorption of DMMP on bulk $WO_3$.[4e] However, there is a lack of detailed understanding on the interaction between DMMP and nanostructured tungsten oxides with structural controls, despite the fact that tungsten oxide nanoclusters are well-known structure-sensitive catalysts.[13] Our previous studies on the decomposition of DMMP on $(MoO_3)_3$ clusters indicated that the adsorption and decomposition of DMMP on metal oxide clusters depend heavily on the Lewis acidity of metal oxides and the oxygen vacancies within the clusters.[12b] Since tungsten oxide clusters are usually used as strong solid acid catalysts industrially,[14] a study of their interaction with DMMP can shed light on the role of the Lewis and Brønsted acidity on both the adsorption and decomposition behaviors of DMMP. The $(WO_3)_3$ clusters were size-selected and soft-landed into a frozen matrix of DMMP multilayers supported on Highly Oriented Pyrolytic Graphite (HOPG) and their interactions with DMMP were studied by spectroscopic tools.

The XPS spectra of P(2p) regions of DMMP on $(WO_3)_3$ are shown in Figure 1. In comparison to previous studies on $(MoO_3)_3$,[12b] the evolution of the P(2p) peak exhibited a similar trend: Initial annealing from room temperature to 200 °C resulted in the shift of P(2p) peak to a lower binding energy, indicating a reduction of phosphorous species; Further annealing to 300 °C did not significantly change the spectral envelope and their intensity; Finally, after annealing to 400 °C, the P(2p) peak shifted slightly back to the higher binding energy, indicating a possible re-oxidation of phosphorous species.

Additionally, during heating, the tungsten oxide was also reduced as indicated by the shift of the W(4f) peak to a lower binding energy as well as the broadening of the spectral envelopes as shown in Figure 2(b). Interestingly, the reduction of $WO_3$ was observed at as low as 200 °C, resulting in the formation of low valency tungsten species. It is suggested that the underlying graphite support may promote the reduction of the $(WO_3)_3$ cluster.[15] It is worth noting that the initial reduction

[a] Dr. X. Tang,[+] Z. Hicks,[+] Dr. K. H. Bowen
Department of Chemistry, Johns Hopkins University, 21218 Baltimore, United States
E-mail: kbowen@jhu.edu
[b] Dr. G. Ganteför
Department of Physics, University of Konstanz, 78464 Konstanz, Germany
[c] Dr. B. W. Eichhorn
Department of Chemistry and Biochemistry, University of Maryland, 20742 College Park, United States
[+] These authors contributed equally to this work.

Supporting information for this article is available on the WWW under https://doi.org/10.1002/slct.201800229

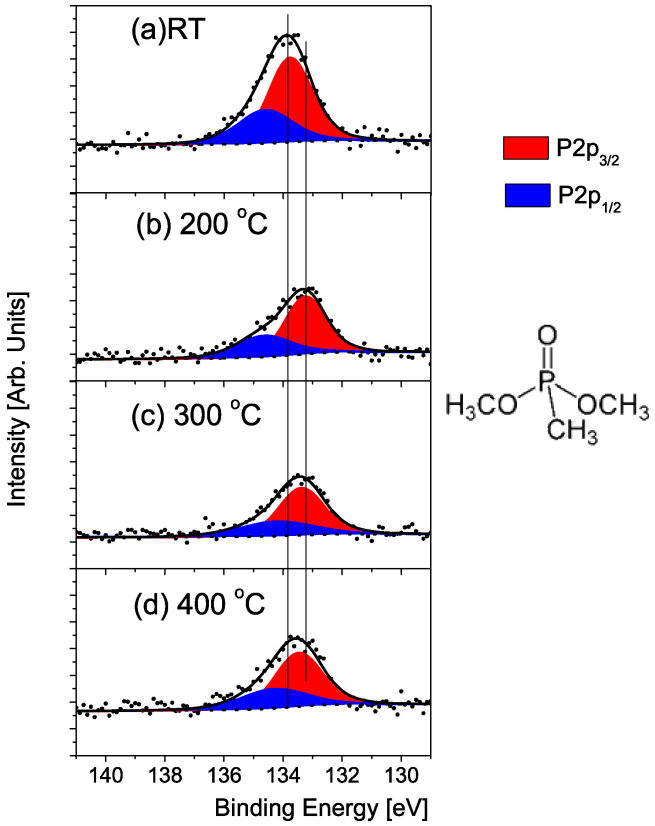


**Figure 1.** P(2p) envelope of DMMP/ $(WO_3)_3$: (a) Room Temperature (b) 200 °C (c) 300 °C (d) 400 °C; The structure of DMMP is shown on the right.

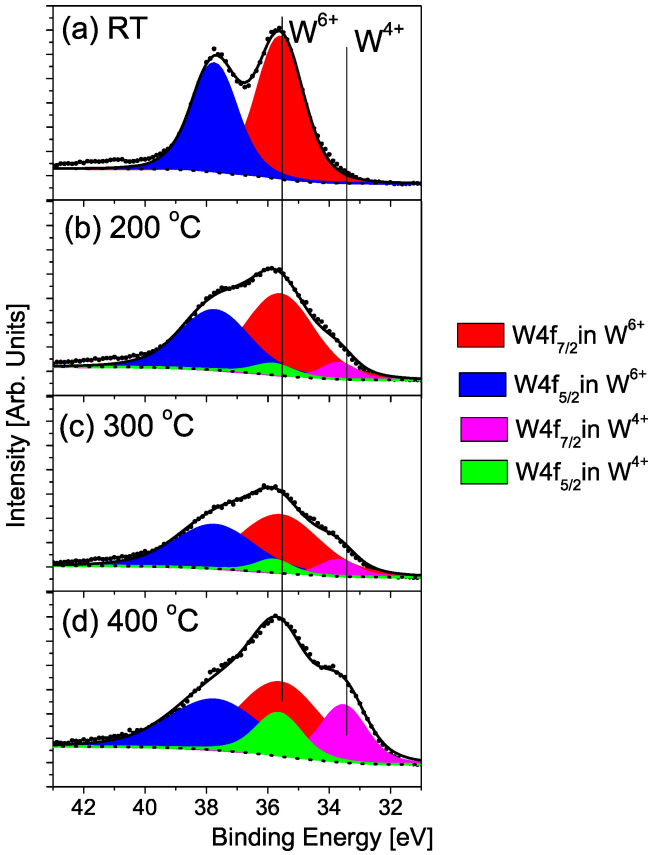


**Figure 2.** W(4f) Envelope of DMMP/ $(WO_3)_3$: (a) Room Temperature (b) 200 °C (c) 300 °C (d) 400 °C

of $WO_3$ appears to synchronize with the reduction of phosphorous species, as indicated in Figure 1. It is known from previous studies on $TiO_2$, that the annealing process introduces the oxygen vacancies as well as conduction band electrons in reducible metal oxides, which act as the active species for reducing phosphorus.[3b]

The loading of DMMP per tungsten atom as a function of the annealing temperature was also calculated and displayed in Figure 3 by dividing the integrated spectral area with the relative sensitivity factor for both W(4f) and P(2p) regions. The initial ratio of P to W was calculated to be 0.33, indicating that only one DMMP molecule can adsorb to each $(WO_3)_3$ cluster. As shown in the plot, the vast majority of DMMP desorbed upon heating to 200 °C, and then remained mostly constant from 200 °C to 300 °C. Further annealing to 400 °C resulted in additional loss of phosphorous species.

The TPR results of DMMP on $(WO_3)_3$ clusters are shown in Figure 4. The intact DMMP was observed to desorb at a lower temperature around 100 °C as shown in the desorption profile at 79 amu, which is the mass of the major fragment of DMMP. This is consistent with the fact that the vast majority of DMMP desorbed between room temperature and 200 °C, as indicated in the XPS experiment (Figure 3). Methanol and dimethyl ether were also observed as major desorption products at higher temperatures. The desorption of dimethyl ether is reflected by the desorption peak around 245 °C at 46 amu, which is the

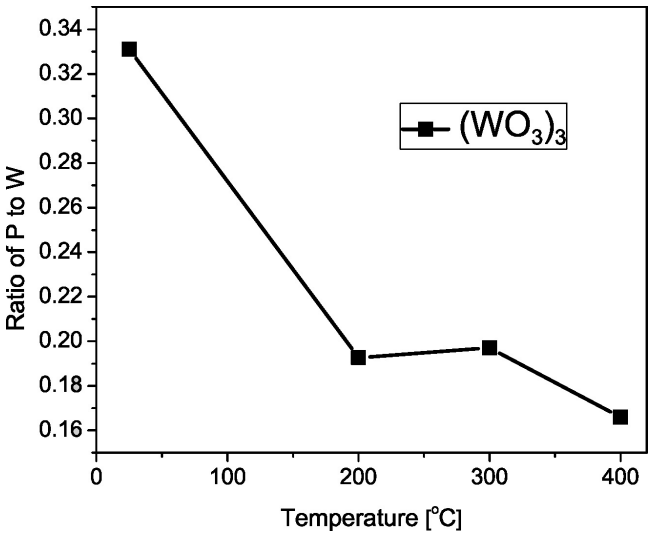


**Figure 3.** Ratio of P to W as a function of the annealing temperature

mass of the parent ion of dimethyl ether. The desorption of methanol is indicated by the desorption peak around 275 °C at both 31 amu and 32 amu. By assuming a frequency factor of $10^{13}$ $s^{-1}$, the desorption energy of DMMP, dimethyl ether and methanol are calculated to be 23.4, 32.8 and 34.8 kcal/mol,

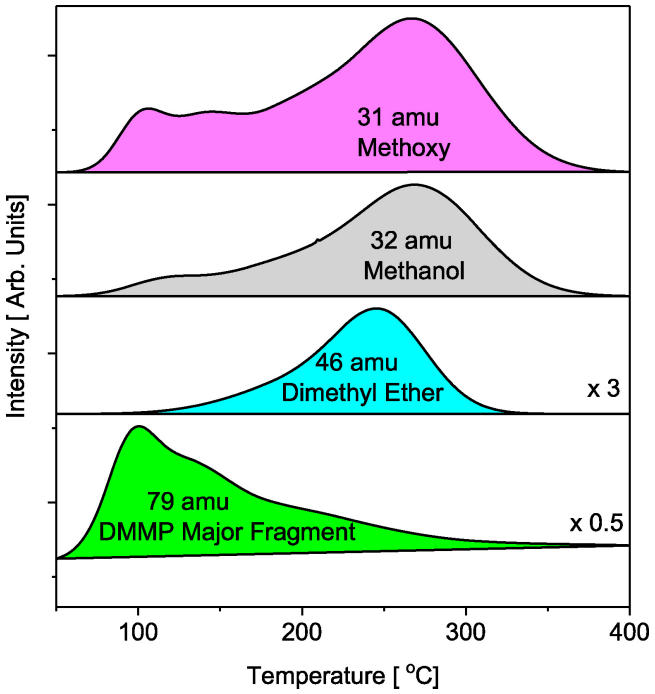


**Figure 4.** TPR Profiles of DMMP on $(WO_3)_3$

respectively, using a simple Redhead analysis.[16] It is suggested by many studies that methoxides are intermediates that lead to the formation of methanol and dimethyl ether.[4f] Therefore, the activation barrier from methoxy to dimethyl ether seems lower than that to methanol.

The adsorption behavior of DMMP on $(WO_3)_3$ is very similar to that on $(MoO_3)_3$ clusters. The interaction between DMMP and $(MO_3)_3$ (M = Mo, W) both resulted in a metal to P ratio of 3:1 at room temperatures, indicating that, for each $(MO_3)_3$ cluster, only one DMMP molecule can adsorb to it. It's suggested by Wang[17] and Dixon[18] that $(WO_3)_3$ and $(MoO_3)_3$ clusters share a similar six-member ring structure and that their electronic structures are comparable. Thus, a similar adsorption geometry and steric interaction with DMMP may be expected for both $(MO_3)_3$ (M = Mo, W) clusters.

The decomposition of DMMP on $(WO_3)_3$ was also revealed by XPS and TPR. As indicated in the XPS studies, reductions of both the phosphorous species and the metal oxides were observed after annealing to 200 °C, which is also similar to DMMP on $(MoO_3)_3$ clusters. Very likely, the reduction of the phosphorous species may have to do with the production of oxygen vacancies, caused by the annealing of metal oxides on the graphite support. Previous studies on both molybdenum oxide thin films and clusters suggested that the oxygen vacancies present on the metal oxide surface may hydroxylate and facilitate both the adsorption and decomposition of DMMP on metal oxides.[5,12] The resulting intermolecular hydrogen transfer between hydroxyls on the cluster and the methoxy groups can lead to the loss of methoxy groups and the formation of methanol, which is supported by *in situ* XPS[5] and TPR[12b] studies. Since the desorption of methanol was also observed for DMMP on $(WO_3)_3$ clusters, the pathway of DMMP on $(WO_3)_3$ may follow a similar route, starting with the thermal annealing of $(WO_3)_3$ clusters, resulting in the formation of reduced tungsten species, i.e. $W^{5+}$ and $W^{4+}$. The reduced metal centers can not only interact with residual water to form surface hydroxyl groups, but also can reduce the phosphorous species in DMMP as indicated in the shift of P(2p) peak to a lower binding energy. It is suggested that methyl methylphosphate (MMP) and methylphosphate (MP) are formed on the oxide surface during the step-loss of the methoxy groups.[19] The production of methanol was also believed to be caused by an intermolecular hydrogen transfer from an adjacent hydroxyl group to methoxides.[19] Further annealing to 400 °C resulted in the P(2p) peak shifting back to a slightly higher binding energy. This is usually attributed to the formation of $PO_x$ species due to the cleavage of P-$CH_3$ bond at higher temperatures.[19]

Moreover, different from that on $(MoO_3)_3$, the formation of dimethyl ether was observed for DMMP on $(WO_3)_3$ clusters. It's well-known that solid acid catalysts can facilitate the dehydration reaction of methanol to dimethyl ether.[20] It is suggested by Neurock and Iglesia that the strong acid catalysts will favor the reaction pathway to dimethyl ether from surface methoxides by stabilizing the transition state to form dimethyl ether.[20b,21] Indeed, the $(WO_3)_3$ cluster is a strong Lewis acid, as indicated by its ability to dehydrate 2-propanol to propene.[22] In addition, the interaction of DMMP and metal oxide surfaces is known to form surface methoxides.[5] Therefore, the stronger Lewis acidity of $(WO_3)_3$ relative to $(MoO_3)_3$ can readily lead to the desorption of dimethyl ether as a consequence of the reaction between DMMP on $(WO_3)_3$ clusters. The different fate of DMMP on these two metal oxide clusters underlined that the difference in Lewis acidity of metal oxide clusters can lead to different product distributions of DMMP possibly by providing different degree of the stabilization of transition states.

In summary, the adsorption behavior and the decomposition pathways of DMMP on $(WO_3)_3$ clusters were studied by *in situ* XPS and TPR. Overall, both the adsorption and the decomposition of DMMP on $(WO_3)_3$ are very similar to that on $(MoO_3)_3$. Only one DMMP molecule can adsorb to each $(WO_3)_3$ cluster. The reduced tungsten species are responsible for decomposing the DMMP molecules. Furthermore, in addition to methanol, dimethyl ether was also observed as the reaction product due to the strong Lewis acidity of $(WO_3)_3$ clusters.

### Supporting Information Summary

The detailed experimental procedures are given in the supporting information.

## Acknowledgements

*This material is based upon work supported by the Defense Threat Reduction Agency (DTRA) under grant number HDTRA1-15-1-0005.*

## Conflict of Interest

The authors declare no conflict of interest.

**Keywords:** DMMP · Tungsten Oxides · Clusters · Lewis Acid · Chemical Warfare Agents

[1] Y. C. Yang, J. A. Baker, J. R. Ward, *Chem. Rev.* **1992**, *92*, 1729–1743.
[2] O. P. Korobeinichev, S. B. Ilyin, T. A. Bolshova, V. M. Shvartsberg, A. A. Chernov, *Combust. Flame* **2000**, *121*, 593–609.
[3] a) A. R. Wilmsmeyer, J. Uzarski, P. J. Barrie, J. R. Morris, *Langmuir* **2012**, *28*, 10962–10967; b) D. A. Panayotov, J. R. Morris, *Langmuir* **2009**, *25*, 3652–3658; c) M. K. Ferguson-McPherson, E. R. Low, A. R. Esker, J. R. Morris, *J. Phys. Chem. B* **2005**, *109*, 18914–18920; d) J. S. Ratliff, S. A. Tenney, X. Hu, S. F. Conner, S. Ma, D. A. Chen, *Langmuir* **2009**, *25*, 216–225; e) S. Ma, J. Zhou, Y. C. Kang, J. E. Reddic, D. A. Chen, *Langmuir* **2004**, *20*, 9686–9694.
[4] a) G. Wang, C. Sharp, A. M. Plonka, Q. Wang, A. I. Frenkel, W. Guo, C. Hill, C. Smith, J. Kollar, D. Troya, J. R. Morris, *J. Phys. Chem. C* **2017**, *121*, 11261–11272; b) Y. Wang, Z. Zhou, Z. Yang, X. Chen, D. Xu, Y. Zhang, *Nanotechnology* **2009**, *20*, 345502; c) D. A. Panayotov, J. R. Morris, *Langmuir* **2009**, *25*, 3652–3658; d) A. Mattsson, C. Lejon, V. Štengl, S. Bakardjieva, F. Opluštil, P. O. Andersson, L. Österlund, *Appl. Catal., B* **2009**, *92*, 401–410; e) S. M. Kanan, A. Waghe, B. L. Jensen, C. P. Tripp, *Talanta* **2007**, *72*, 401–407; f) M. B. Mitchell, V. N. Sheinker, W. W. Cox, E. N. Gatimu, A. B. Tesfamichael, *J. Phys. Chem. B* **2004**, *108*, 1634–1645.
[5] A. R. Head, R. Tsyshevsky, L. Trotochaud, Y. Yu, L. Kyhl, O. Karslıoğlu, M. M. Kuklja, H. Bluhm, *J. Phys. Chem. C* **2016**, *120*, 29077–29088.
[6] S. Ma, J. Zhou, Y. C. Kang, J. E. Reddic, D. A. Chen, *Langmuir* **2004**, *20*, 9686–9694.
[7] L. Trotochaud, R. Tsyshevsky, S. Holdren, K. Fears, A. R. Head, Y. Yu, O. Karslıoğlu, S. Pletincx, B. Eichhorn, J. Owrutsky, J. Long, M. Zachariah, M. M. Kuklja, H. Bluhm, *Chem. Mater.* **2017**, *29*, 7483–7496.
[8] Y. X. Li, K. J. Klabunde, *Langmuir* **1991**, *7*, 1388–1393.
[9] Y. Paukku, A. Michalkova, J. Leszczynski, *J. Phys. Chem. C* **2009**, *113*, 1474–1485.
[10] W. O. Gordon, B. M. Tissue, J. R. Morris, *J. Phys. Chem. C* **2007**, *111*, 3233–3240.
[11] D. A. Trubitsyn, A. V. Vorontsov, *J. Phys. Chem. B* **2005**, *109*, 21884–21892.
[12] a) A. R. Head, X. Tang, Z. Hicks, L. Wang, H. Bleuel, S. Holdren, L. Trotochaud, Y. Yu, L. Kyhl, O. Karslıoğlu, K. Fears, J. Owrutsky, M. Zachariah, K. H. Bowen, H. Bluhm, *Catal. Struct. React.* **2017**, *3*, 112–118; b) X. Tang, Z. Hicks, L. Wang, G. Ganteför, K. H. Bowen, R. Tsyshevsky, J. Sun, M. M. Kuklja, *Phys. Chem. Chem. Phys.* **2018**, *20*, 4840–4850.
[13] D. G. Barton, M. Shtein, R. D. Wilson, S. L. Soled, E. Iglesia, *J. Phys. Chem. B* **1999**, *103*, 630–640.
[14] D. G. Barton, S. L. Soled, E. Iglesia, *Top. Catal.* **1998**, *6*, 87–99.
[15] X. Tang, K. H. Bowen, F. Calvo, *Phys. Chem. Chem. Phys.* **2017**, *19*, 31168–31176.
[16] P. A. Redhead, *Vacuum* **1962**, *12*, 203–211.
[17] X. Huang, H. J. Zhai, B. Kiran, L. S. Wang, *Angew. Chem. Int. Ed.* **2005**, *44*, 7251–7254.
[18] S. Li, D. A. Dixon, *J. Phys. Chem. A* **2006**, *110*, 6231–6244.
[19] D. A. Chen, J. S. Ratliff, X. Hu, W. O. Gordon, S. D. Senanayake, D. R. Mullins, *Surf. Sci.* **2010**, *604*, 574–587.
[20] a) F. Yaripour, F. Baghaei, I. Schmidt, J. Perregaard, *Catal. Commun.* **2005**, *6*, 147–152; b) W. Alharbi, E. F. Kozhevnikova, I. V. Kozhevnikov, *ACS Catal.* **2015**, *5*, 7186–7193.
[21] a) R. T. Carr, M. Neurock, E. Iglesia, *J. Catal.* **2011**, *278*, 78–93; b) A. J. Jones, R. T. Carr, S. I. Zones, E. Iglesia, *J. Catal.* **2014**, *312*, 58–68.
[22] X. Tang, D. Bumueller, A. Lim, J. Schneider, U. Heiz, G. Ganteför, D. H. Fairbrother, K. H. Bowen, *J. Phys. Chem. C* **2014**, *118*, 29278–29286.

Submitted: January 25, 2018
Revised: March 9, 2018
Accepted: March 12, 2018